Carbohydrate Research 533 (2023) 108938

Contents lists available at ScienceDirect

Carbohydrate Research

journal homepage: www.elsevier.com/locate/carres

Tyrosine glucosylation of collagen films exploiting Horseradish Peroxidase (HRP)

Francesca Cadamuro [a], Matteo Ferrario [a], Raziyeh Akbari [b], Carlo Antonini [b], Francesco Nicotra [a], Laura Russo [a,c,*]

[a] School of Medicine and Surgery, University of Milano-Bicocca, 20854, Vedano al Lambro, Italy
[b] Department of Materials Science, University of Milano-Bicocca, 20126, Milan, Italy
[c] CÚRAM, SFI Research Centre for Medical Devices, National University of Ireland Galway, H91TK33, Galway, Ireland

ARTICLE INFO

Keywords:
Biomaterials glycosylation
Collagen
HRP
Glycosignature

ABSTRACT

The development of human tissue models for regenerative medicine and animal-free drug screening requires glycosylated biomaterials such as collagen. An easy and fast biomaterial glycosylation method exploiting Horseradish Peroxidase (HRP) phenol coupling reaction is proposed. The protocol is adaptable to any polymer functionalized with phenol residues or tyrosine containing proteins. As a model the tyrosine residues on collagen films were functionalized with salidroside, a natural β-glucoside with a phenol in the aglycone. Scanning Electron Microscope (SEM) and contact angle analysis revealed the influence of glycosylation on the sample's morphology and wettability. Preliminary biological evaluation showed the cytocompatibility of the glucosylated collagen films.

1. Introduction

Biomaterials glycosylation is fundamental to generate *in vitro* tissue models suitable to study the role of the extracellular matrix (ECM) in human pathologies and to develop personalized therapeutic strategies [1–4]. Indeed, the mechanism by which glycans of the ECM influence cell fate is still largely unclear, requiring efforts to generate libraries of glycoengineered tissue models with different properties and study the impact on cell behaviour [5,6]. To this purpose it is necessary to develop and validate new methods for biomaterials glycosylation, ideally milder with respect to those already explored in literature such as reductive amination and chemo selective ligations [7–10]. In this contest, we considered the possibility to exploit the HRP phenol coupling reaction [11], as easy and fast conjugation method adaptable to any polymer containing a phenol residue, among which proteins with tyrosine residues.

We selected collagen as biomaterial, being the main component of the ECM. Collagen contains ~0.5% of tyrosine residues, mainly exposed and therefore suitable for functionalization [12]. As a model of monosaccharide, we selected salidroside, a commercially available β-glucoside of tyrosol found in the plant Rhodiola rosea. The approach, of course, can be extended to any monosaccharide with a phenol in the aglycone.

Collagen films were reacted with salidroside upon activation of HRP with hydrogen peroxide in physiological conditions. The reaction was selective and proceed at room temperature in Phosphate-buffered saline (PBS) at pH 7.4. Furthermore, this protocol exploiting the tyrosine residues of collagen, doesn't modify other amino acids involved in pH regulation and cell adhesion processes.

2. Materials and method

2.1. Materials

Collagen from bovine Achilles tendon (Sigma Aldrich, C9879), acetic acid, PBS, HRP, oxygen peroxide, sulfuric acid, Dulbecco's modified Eagle's medium, fetal bovine serum, penicillin, streptomycin, bovine serum albumin (BSA), formalin, Triton X were purchased from Sigma-Aldrich. Ethanol was purchased from Honeywell. AlamarBlue™ Cell Viability Reagent, Alexa Fluor 647 Phalloidin, 4′,6-diamidino-2-phenylindole (DAPI), Concanavalin A (ConA) (Alexa Fluor™ 594 Conjugate solution), Peanut agglutinin (PNA) from arachis hypogaea (Alexa

* Corresponding author. School of Medicine and Surgery, Via Raoul Follereau 3, 20854, Vedano al Lambro, MB, Italy.
E-mail addresses: francesca.cadamuro@unimib.it (F. Cadamuro), m.ferrario@campus.unimib.it (M. Ferrario), raziyeh.akbari@unimib.it (R. Akbari), carlo.antonini@unimib.it (C. Antonini), francesco.nicotra@unimib.it (F. Nicotra), laura.russo@unimib.it (L. Russo).

https://doi.org/10.1016/j.carres.2023.108938
Received 16 June 2023; Received in revised form 31 August 2023; Accepted 1 September 2023
Available online 9 September 2023

Fluor™ 488 Conjugate solution) from Thermo Fisher Scientific; Salidroside from Rhodiola rosea from Carbosynth Ltd; Human glioblastoma cell line U87 from LGC Standards S.r.L.

2.2. Collagen film preparation

Collagen films were prepared by solvent casting as previously reported in literature [13]. Briefly, 690 mg of collagen were solubilized by stirring in 315 mL acetic acid 0.5 M for 1 h at 40 °C. The suspension was homogenized with a mixer for 2 min at maximum speed. 60 mL of the solution were transferred in a flat polystyrene mould with a syringe and left to dry for 48 h. The resulting films were gently detached from polystyrene moulds using deionized water and a spatula, washed with a 0.1 M solution of NaCl, then three times with deionized water and finally immersed in EtOH and left to dry.

2.3. Functionalization of collagen films with salidroside

Two collagen films (11,7 × 7,5 cm, 83 mg each) were enzymatically functionalized with salidroside. Both films were previously cleaned with ethanol to remove possible contaminants. The reaction was performed in 12 × 8 cm box, designed to avoid folding of the sides during the constant agitation of the solution. Salidroside (69 mg, 0.228 mmol) was dissolved in 25 mL of pH 7.4 PBS, and this solution was used to cover the films. Solutions of HRP and subsequently H_2O_2 were added to reach a total volume of 25 mL and a final concentration of 0.1 U/mL HRP, 0.001 mM H_2O_2. The reaction was stirred for 2 and 3 h at rt. The films were then washed with NaCl saturated water, followed by MilliQ and lastly with EtOH 70% to dehydrate and distend them, covered by aluminium foil.

2.4. Contact angle

The contact angle measurement in static and quasi-static modes were carried out on 1 cm × 1 cm collagen film samples at room temperature using a home-made set-up including a high-speed camera (PHOTRON-NOVA FASTCAM S6, 2:1 Venus Laowa 100 mm f/2.8 2X Ultra Macro APO lens, JJC Auto Focus Extension Tube 20 mm, pixel size = 9 μm). In static contact angle measurements, a 5 μL distilled water droplet was placed gently on the sample. In quasi-static measurements, water drop was infused and withdrawn from the sample surface in a rate of 10 μL/min to measure the advancing and receding contact angles. Three measurements were performed on both untreated (as control) and functionalized collagen films and analysed by Dropen software [14].

2.5. SEM

The morphology and microstructure were evaluated by scanning electron microscopy using a ZEISS Gemini 500 field emission HR-SEM at voltage of 5 kV. 0.5 cm × 0.5 cm collagen film adhered to a glass slide. The samples were fixed with conductive adhesive on aluminium supports, and then coated with graphite.

2.6. UV–vis analysis

1 cm × 1 cm Collagen film samples were attached to a glass slide and analysed with a UV–Vis Jasco V-770 spectrometer with single monochromator and double beam type. An empty glass slide was used as blank. Spectra were collected between 190 and 700 nm with a scanning speed of 100 nm/min.

2.7. Lectin-based assay

The protocol was adapted from Ref. [15]. 1 cm × 1 cm collagen film samples were incubated overnight with 2% BSA in PBS in 24 well plate at 4 °C. Then the BSA solution was removed, and the films were incubated for 2 h with 0.01 mg/mL Concanavalin A, Alexa Fluor™ 594 Conjugate solution in PBS pH 7.4 at room temperature with gentle shaking. The samples were thoroughly washed three times with PBS pH 7.4. The assay was performed in three replicates for each condition. Fluorescence images were collected with CELENA®S, Logos Biosystems. The protocol has been replicate using PNA from arachis hypogaea (Alexa Fluor™ 488 Conjugate solution) with a concentration of 0.01 mg/mL.

2.8. Anthrone assay

To assert the degree of glucosylation of the collagen, anthrone assay was performed (protocol adapted from Ref. [16]). 20 mg of anthrone powder were dissolved in concentrated H_2SO_4 to a final concentration of 0.2% w/V. 5 mg of both treated and untreated films (circa 1 cm × 2 cm) were hydrated with 100 μL of MilliQ H_2O, followed by 400 μL of anthrone solution; the reaction was kept at 90 °C for 10 min. 100 μL of each final solution were posed into 96-microwell plates and the absorbance values (620 nm) measured with UV–Vis SPECTROstar Nano BMG LABTECH. The assay was performed in triplicate.

2.9. Analytical instruments FT-IR

FT-IR spectra were performed with dry film using a Nicolet iS20, Thermo Scientific.

2.10. In vitro tests

2.10.1. Human U87 glioblastoma cells

Human glioblastoma U87 cells were cultured in Dulbecco's modified Eagle's medium supplemented with 10% fetal bovine serum, 100 units/mL penicillin, and 100 mg/mL streptomycin at 37 °C under a humidified atmosphere with 5% CO_2. Cells were grown to 90% confluence, trypsinized, plated in 75 cm^2 culture dishes at a density of 1.5×10^6 cells and incubated at 37 °C in a humidified atmosphere containing 5% CO_2. The medium was changed every three days.

2.10.2. Fluorescence analysis

1 cm × 1 cm collagen film samples were placed in a 48 well plate and sterilized under UV for 30 min. Then films were hydrated with Dulbecco's modified Eagle's medium for 30 min at 37 °C. 15000 cells/well were cultured on the films for 7 days. After fixation with 10% formalin the films were washed three times with PBS, then permeabilized with 0.3% (w/v) Triton X solution, and stained with 0.66 μg/mL of phalloidin and 0.4 μg/mL of DAPI. Fluorescence images were collected with CELENA®S, Logos Biosystems, where the blue and red colours indicated the nuclei and actin cytoskeleton respectively.

2.10.3. Alamar blue assay

Samples with a diameter of 0.5 cm were placed in a 96 wellplate and sterilized under UV for 30 min. Then films were hydrated with Dulbecco's modified Eagle's medium for 30 min at 37 °C. 5000 cells/well were cultured on the films for 7 days. Positive and negative control was obtained by cells growing on the well plate, without films. DMSO was used to kill the cells of negative control. After 24, 48, and 72 h the medium was replaced with 10% Alamar blue solution in Dulbecco's modified Eagle's medium, and incubate for 2h. Supernatant solution was collected and absorbance values (570 and 600 nm) measured with UV–Vis SPECTROstar Nano BMG LABTECH. The percentage of alamar reduction was calculated as:

AO_{LW} = absorbance of AlamarBlue in media at 570 nm - absorbance of media only

AO_{HW} = absorbance of AlamarBlue in media at 600 nm - absorbance of media only

$R_O = AO_{LW} / AO_{HW}$

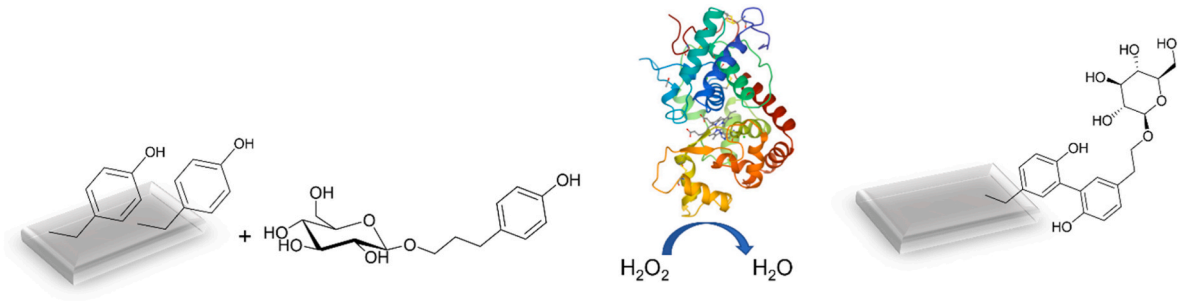

Scheme 1. Schematic representation of the reaction catalysed by HRP to conjugate salidroside and collagen films (adapted from Ref. [18]).

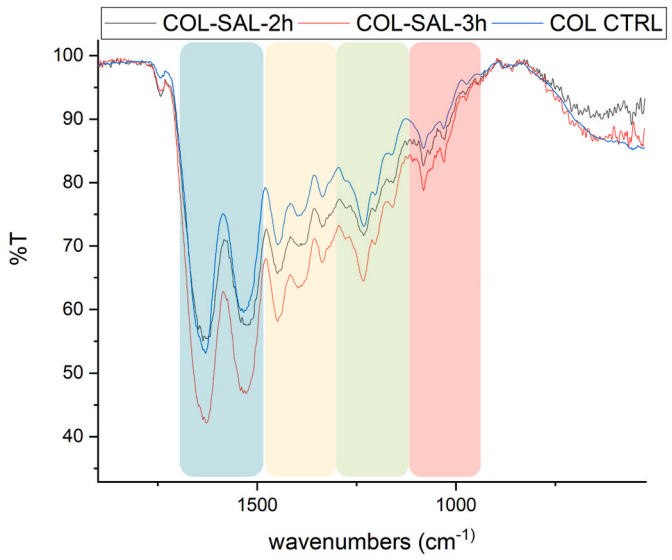

Fig. 1. FT-IR spectra of COL-SAL-2h (black), COL-SAL-3h (red) and COL CTRL (blue).

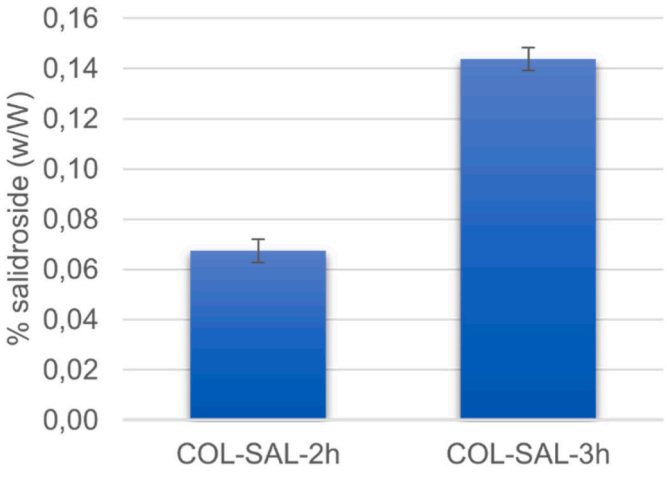

Fig. 2. Quantification of the degree of functionalization of COL-SAL-2h and COL-SAL-3h.

A_{LW} = absorbance at the lower wavelength – absorbance of media only

A_{HW} = absorbance at the higher wavelength – absorbance of media only

Percentage difference in reduction = A_{LW} - (A_{HW} x R_O) x 100

3. Results and discussion

3.1. Chemical modifications of collagen films with salidroside

In this work a simple and fast enzymatic approach to functionalize an ECM structural protein such as collagen with monosaccharides has been developed. The proposed chemoselective approach demonstrates to be effective under mild conditions, avoiding prior surface modification of collagen. Noteworthy, the tyrosine residues are usually exposed at the collagen surface, and tyrosine phosphorylation and GlcNAcylation are dynamic post-translational modification occurring in some proteins, with conformational and functional changes.

We exploited HRP to catalyse an oxidative phenol-phenol coupling between the tyrosine residues (0.5% w/W) of collagen films and the phenol of salidroside [17] (Scheme 1). Two different timelines of the reactions were tested to obtain different degree of functionalization. In the first one the coupling reaction was stopped after 2 h (COL-SAL-2h), while in the second one was left to proceed for 3 h (COL-SAL-3h). The functionalization degree of the two samples was determined, using unmodified collagen film as control (COL CTRL).

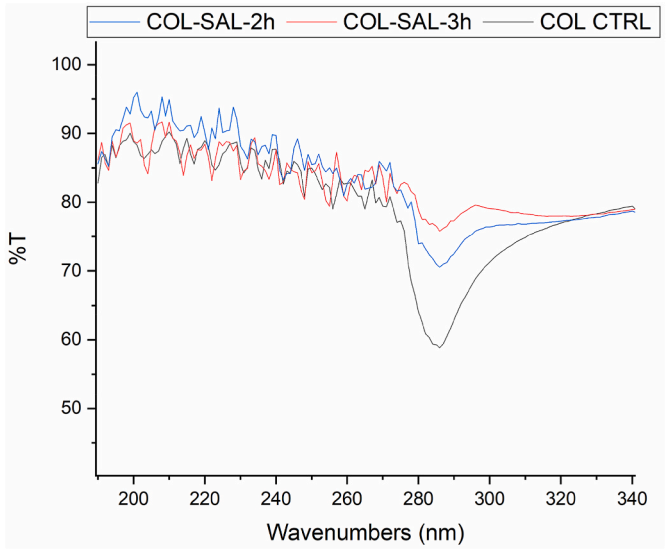

Fig. 3. UV-VIS spectra of COL-SAL-2h (blue), COL-SAL-3h (red) and COL CTRL (black).

3.2. Characterization of glycosylated film

FT-IR. The FT-IR spectra of COL-SAL-2h, COL-SAL-3h, in comparison to the unmodified collagen film COL CTRL as control are reported in Fig. 1. FT-IR spectra of collagen exhibits for all the analysed samples characteristic absorptions bands of amide I and amide II (highlighted in blue ~1650 cm^{-1} and ~1500 cm^{-1}), weaker absorptions bands of amide

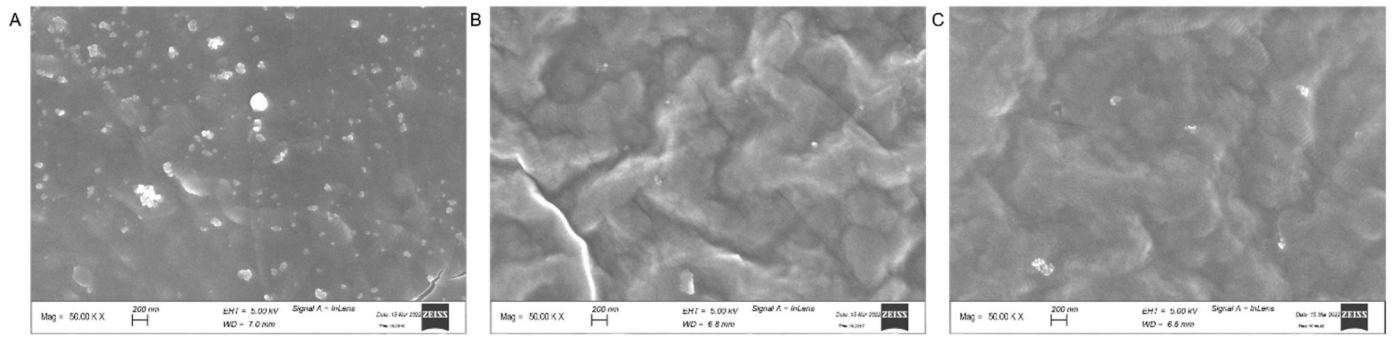

Fig. 4. SEM images of A) COL CTRL, B) COL-SAL-2h and C) COL-SAL-3h. Scale bar 200 μm.

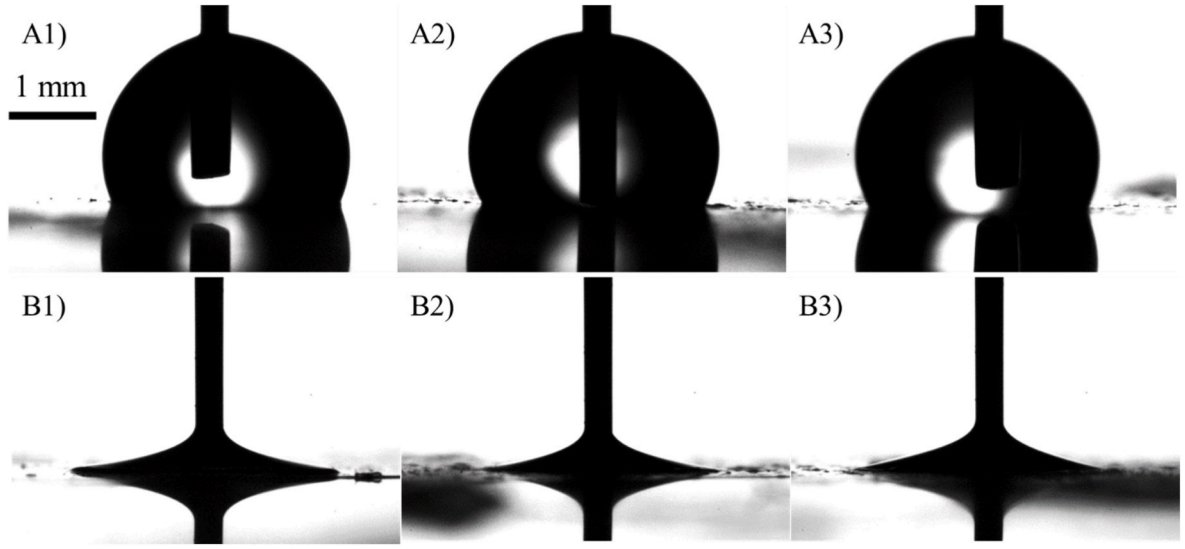

Fig. 5. Images from the advancing contact angles on A1) COL CTRL, A2) COL-SAL-2h and A) COL-SAL-3h. Images from the receding **c**ontact angles on B1) COL CTRL, B2) COL-SAL-2h and B3) COL-SAL-3h.

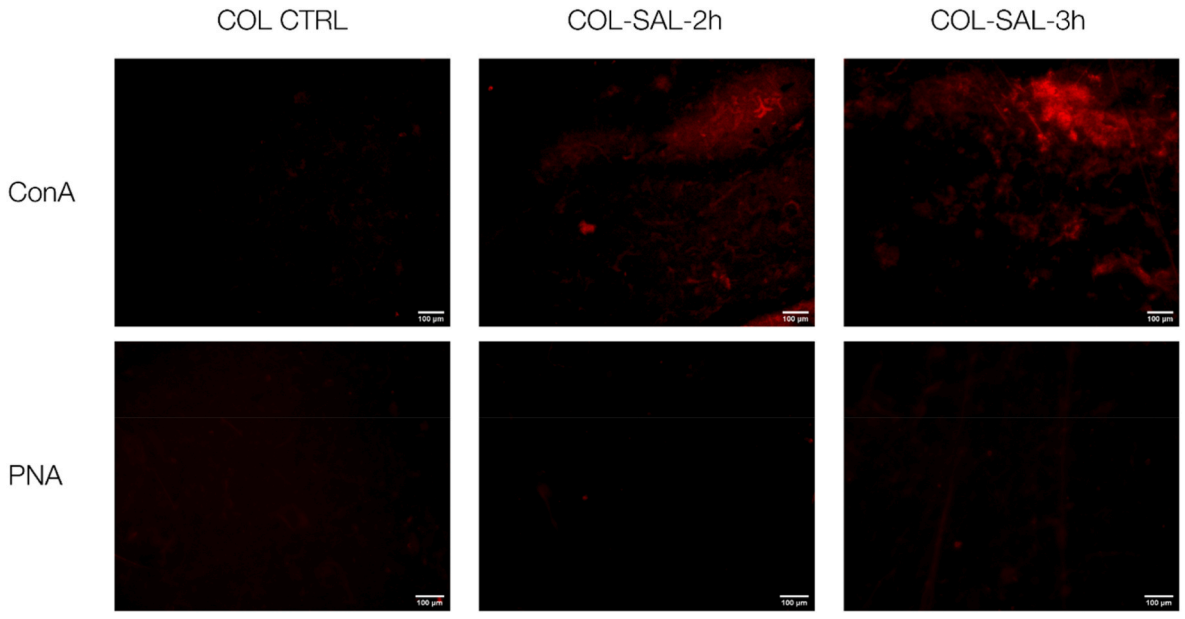

Fig. 6. A) Fluorescence images of COL CTRL, COL-SAL-2h and COL-SAL-3h with PNA–Alexa fluor™ 488 (top) and ConA - Alexa Fluor™ 594 (bottom). Scale bar 100 μm.

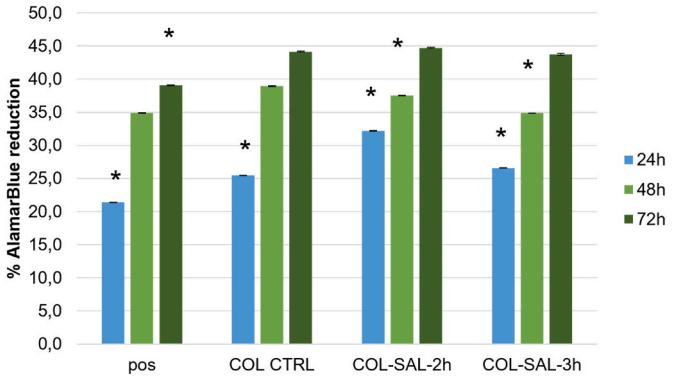

Fig. 7. Alamar blue assay of cells cultured on the treated well plate as positive control (pos), cells cultured on top of COL CTRL, COL-SAL-2h and COL-SAL-3h. Data are presented as means ± SD of three experiments. *p < 0.05, **p < 0.01.

III (highlighted in green ~1245 cm−1 cm^{-1}) and adsorptions bands of δ(CH_2), and δ(CH_3) (highlighted in yellow ~1480–1350 cm^{-1}) [19,20]. The functionalization of both COL-SAL-2h, COL-SAL-3h was confirmed by the presence of the characteristic peaks of salidroside. C–O–C stretching vibration and C–O stretching vibration were visible respectively between 1200 and 900 cm^{-1} (highlighted in red [21,22]).

Anthrone assay. The degree of functionalization of COL-SAL-2h, COL-SAL-3h was determined by Anthrone assay. The final concentration of Salidroside attach to collagen film can be influenced by the concentration of HRP, H_2O_2, substrate and duration of the reaction [23,24]. In this work we compared different timelines of the reaction keeping constant the other parameters. The concentration of salidroside in COL-SAL-3h resulted 0,014% (w/W), while in COL-SAL-2h resulted 0,07% (w/W) (Fig. 2) corresponding to a degree of functionalization of tyrosine residues respectively of 28% and 14%.

UV-VIS. UV–Vis spectra of COL-SAL-2h, COL-SAL-3h and COL CTRL were acquired (Fig. 3). At 280 cm^{-1} the intensity of the peak related to the absorbance of tyrosine gradually decreases with the increase of functionalization, probably due to a quenching effect as reported in literature for similar cases [25].

SEM. Protein glycosylation has impacts not only in the biological activity but also the final molecular structure, as largely studied in the literature [4,26,27]. The SEM analysis of the glucosylated films COL-SAL-2h and COL-SAL-3h showed an increase in the tendency to form ordered structures in comparison to COL CTRL (Fig. 4). Indeed it is possible to appreciate short native fibrils, similar to what was observed in neoglycosylated collagen films reported in literature [22,28–30].

Contact angle. Wettability of the glucosylated collagen films was evaluated by a contact angle sessile drop method. COL CTRL, COL-SAL-2h and COL-SAL-3h samples have a static contact angle of 90° ± 2°, 82° ± 2°, and 90° ± 2°, respectively, i.e. at the threshold between a hydrophilic and hydrophobic behaviour. A single value of the contact angles, especially on complex surfaces, do not necessarily provide a correct understanding of the wetting behaviour. This is why it is important to perform more careful complete quasi-static wetting experiments, measuring both advancing (Fig. 5 A1-3) and receding contact angles (Fig. 5 B1-3). Indeed, tests show that all the three samples have comparable advancing contact angles values, with initial relatively hydrophobic values, i.e. COL CTRL 110° ± 9° (Fig. 5 A1), COL-SAL-2h 116° ± 1° (Fig. 5 A2), and COL-SAL-3h 117° ± 3° (Fig. 5 A3); however, samples become hydrophilic after drop deposition, due to the high tendency of the collagen surfaces to absorb water: as a result, the receding contact angles are low (<20°) (see Fig. 5 B1-3).

Lectin-based assay. Lectins-based assay was used to assess the functionalization of collagen films and the exposition of glucose for biological recognitions (Fig. 6). Even if ConA is used to recognise α-D-glucosyl residues, it is known that the presence of an aromatic entity as aglycone results in the recognition of β-D-glucosides [19], and therefore is suitable to detect the salidroside residue. The samples were treated with a 2% BSA blocking solution to avoid non-specific binding and then incubated with ConA, (Alexa Fluor™ 594 Conjugate solution) and PNA (Alexa Fluor™ 488 Conjugate solution) [15]. COL CTRL resulted negative to both staining, as expected. Glucosylated films resulted both positive of the ConA staining, and COL-SAL-3h showed slightly higher fluorescence with respect to COL-SAL-2h, as expected. As negative control, the samples were incubated with PNA, which is selective for galactosyl (β-1,3) *N*-acetyl-galactosamine structures.

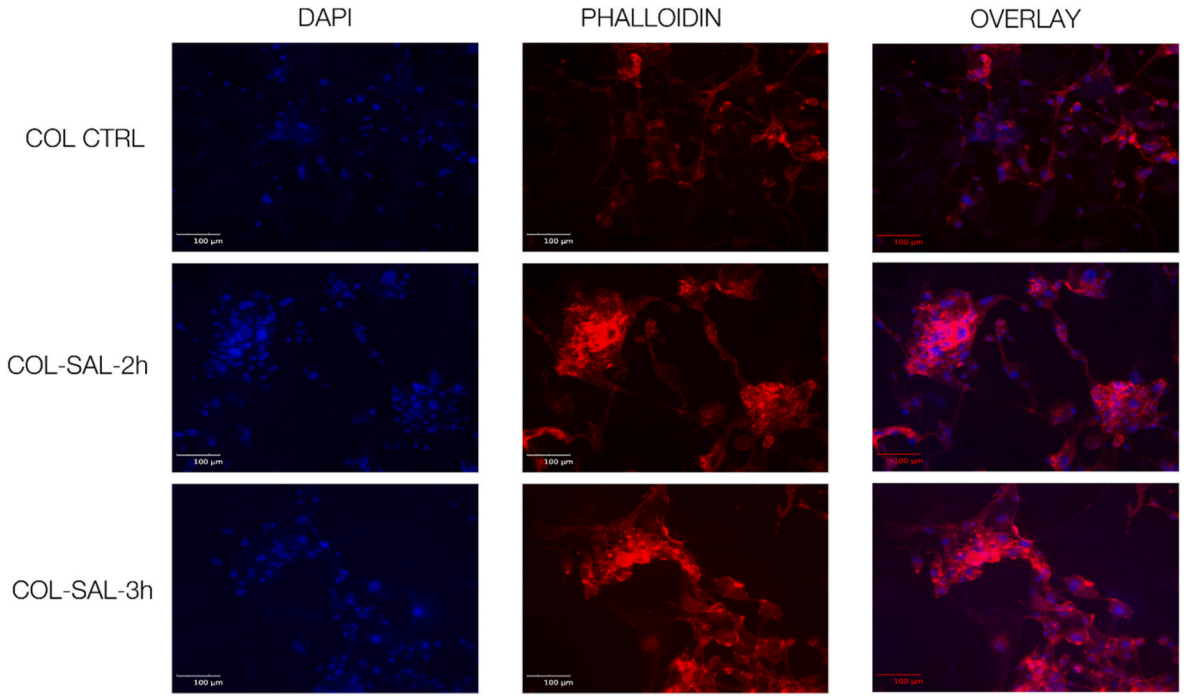

Fig. 8. Fluorescence images of Phalloidin – DAPI staining of film COL CTRL, COL-SAL-2h and COL-SAL-3h. Scale bar 100 μm.

3.3. Biological characterization

Viability. COL CTRL, COL-SAL-2h, and COL-SAL-3h were tested with Alamar blue assay to check the viability of U87 cells. As reported in Fig. 7 Alamar reduction was higher for cells plated on the three films with respect to the positive control, in which cells growth on the treated well plate. Therefore, the functionalized films resulted not cytotoxic. It is noteworthy that salidroside alone inhibits the growth of U87 cells [26] whereas, once involved in the conjugation, the phenolic pharmacophore is lost.

Morphological analysis. Cell morphologies on the films were examined using Phalloidin to highlight the cytoskeleton (red fluorescence) and DAPI (blue fluorescence) to visualize the nuclei (Fig. 8). After 7 days of cell culture in both glucosylated samples a higher number of cells were visible and they were organized in clusters, while in COL CTRL cells appeared more spread and not organized.

4. Conclusion

The design and validation of new strategies to glyco-functionalized biomaterials is fundamental to develop *in vitro* tissue model able to mimic the native crosstalk between cells and ECM. These models are essential to study the mechanisms leading to human pathologies and design new therapies. This work proposes an adaptable protocol for easy and fast glycosylation of collagen films exploiting an HRP catalysed oxidative coupling between the tyrosine residues of the protein and a phenol residue of a glycosyl aglycon. The use of biocatalyst allows to easily obtain the product without side products, use of toxic reagent or toxic solvents. The reaction was successfully experimented with commercially available salidroside, a β-D-glucoside containing a phenolic aglycon, but the application can be extended to other glycans containing a phenol appendage. The degree of functionalization can be tuned controlling the experimental conditions, in our case resulted 28% and 14% in COL-SAL-3h and COL-SAL-2h respectively. The glucosylated collagen films resulted highly biocompatible and, with respect to the control (collagen film) a higher number of cells were visible, and they were well organized in clusters. In conclusion, the glycoconjugate collagen easily and sustainably obtained by enzymatic approach, is a suitable candidate for application in tissue engineering.

Declaration of competing interest

The authors declare that they have no known competing financial interests or personal relationships that could have appeared to influence the work reported in this paper.

Data availability

Data will be made available on request.

Acknowledgements

The authors acknowledge Dr. Paolo Gentile for SEM analysis.

This work was funded by: COST Action CA18132 - Functional Glyconanomaterials for the Development of Diagnostics and Targeted Therapeutic Probes (GLYCONanoPROBES); Italian Ministry of Health (Grant No. RF-2016-02362946); the National Plan for NRRP Complementary Investments in the call for the funding of research initiatives for technologies and innovative trajectories in the health and care sectors - project AdvaNced Technologies for Human-centrEd Medicine (ANTHEM) CUP: B53C22006670001.

References

[1] S. Sampaolesi, F. Nicotra, L. Russo, Glycans in nanomedicine, impact and perspectives, Future Med. Chem. 11 (2019) 43–60, https://doi.org/10.4155/fmc-2018-0368.

[2] A.L. Rebelo, J. Bizeau, L. Russo, A. Pandit, Glycan-functionalized collagen hydrogels modulate the glycoenvironment of a neuronal primary culture, Biomacromolecules 21 (2020) 2681–2694, https://doi.org/10.1021/acs.biomac.0c00387.

[3] F. Barbugian, F. Cadamuro, S. Magli, F. Nicotra, L. Rossi, L. Russo, Diagnostic glycotools, carbohydr, Chem 45 (2021) 572–608, https://doi.org/10.1039/9781839164538-00572.

[4] F. Cadamuro, L. Marongiu, M. Marino, N. Tamini, L. Nespoli, N. Zucchini, A. Terzi, D. Altamura, Z. Gao, C. Giannini, G. Bindi, A. Smith, F. Magni, S. Bertini, F. Granucci, F. Nicotra, L. Russo, 3D bioprinted colorectal cancer models based on hyaluronic acid and signalling glycans, Carbohydr. Polym. 302 (2023), 120395, https://doi.org/10.1016/J.CARBPOL.2022.120395.

[5] J.E. Hudak, C.R. Bertozzi, Glycotherapy: New Advances Inspire a Reemergence of Glycans in Medicine, (n.d.). https://doi.org/10.1016/j.chembiol.2013.09.010.

[6] J.E. Hudak, H.H. Yu, C.R. Bertozzi, Protein glycoengineering enabled by the versatile synthesis of aminooxy glycans and the genetically encoded aldehyde tag, J. Am. Chem. Soc. 133 (2011) 16127–16135, https://doi.org/10.1021/JA206023E.

[7] B. Sarkar, N. Jayaraman, Glycoconjugations of biomolecules by chemical methods, Front. Chem. 8 (2020) 888, https://doi.org/10.3389/fchem.2020.570185.

[8] C. Gardelli, L. Russo, L. Cipolla, M. Moro, F. Andriani, O. Rondinone, F. Nicotra, G. Sozzi, G. Bertolini, L. Roz, Differential glycosylation of collagen modulates lung cancer stem cell subsets through β1 integrin-mediated interactions, Cancer Sci. 112 (2021) 217–230, https://doi.org/10.1111/cas.14700.

[9] F. Cadamuro, F. Nicotra, L. Russo, 3D printed tissue models: from hydrogels to biomedical applications, J. Contr. Release 354 (2023) 726–745, https://doi.org/10.1016/J.JCONREL.2023.01.048.

[10] F. Cadamuro, L. Russo, F. Nicotra, Biomedical hydrogels fabricated using diels alder crosslinking, Eur. J. Org Chem. n/a (n.d.). https://doi.org/doi:10.1002/ejoc.202001042.

[11] B. Tang, Y. Wang, H. Liang, Z. Chen, X. He, H. Shen, Studies on the oxidation reaction of tyrosine (Tyr) with H2O2 catalyzed by horseradish peroxidase (HRP) in alcohol–water medium by spectrofluorimetry and differential spectrophotometry, Spectrochim. Acta Part A Mol. Biomol. Spectrosc. 63 (2006) 609–613, https://doi.org/10.1016/J.SAA.2005.06.008.

[12] S. Jus, I. Stachel, W. Schloegl, M. Pretzler, W. Friess, M. Meyer, R. Birner-Gruenberger, G.M. Guebitz, Cross-linking of collagen with laccases and tyrosinases, Mater. Sci. Eng., C 31 (2011) 1068–1077, https://doi.org/10.1016/J.MSEC.2011.03.007.

[13] A. Sgambato, L. Russo, M. Montesi, S. Panseri, M. Marcacci, E. Caravà, M. Raspanti, L. Cipolla, Different sialoside epitopes on collagen film surfaces direct mesenchymal stem cell fate, ACS Appl. Mater. Interfaces 8 (2016) 14952–14957, https://doi.org/10.1021/acsami.5b08270.

[14] R. Akbari, C. Antonini, Contact angle measurements: from existing methods to an open-source tool, Adv. Colloid Interface Sci. 294 (2021), 102470, https://doi.org/10.1016/J.CIS.2021.102470.

[15] A.M. Slaney, V.A. Wright, P.J. Meloncelli, K.D. Harris, L.J. West, T.L. Lowary, J. M. Buriak, Biocompatible carbohydrate-functionalized stainless steel surfaces: a new method for passivating biomedical implants, ACS Appl. Mater. Interfaces 3 (2011) 1601–1612, https://doi.org/10.1021/am200158y.

[16] T.A. Scott, E.H. Melvin, Determination of dextran with anthrone, Anal. Chem. 25 (1953) 1656–1661, https://doi.org/10.1021/ac60083a023.

[17] L. Russo, A. Sgambato, M. Lecchi, V. Pastori, M. Raspanti, A. Natalello, S.M. Doglia, F. Nicotra, L. Cipolla, Neoglucosylated collagen matrices drive neuronal cells to differentiate, ACS Chem. Neurosci. 5 (2014) 261–265, https://doi.org/10.1021/am200158y.

[18] G.H. Carlsson, P. Nicholls, D. Svistunenko, G.I. Berglund, J. Hajdu, Complexes of horseradish peroxidase with formate, acetate, and carbon monoxide, Biochemistry 44 (2005) 635–642, https://doi.org/10.1021/bi0483211.

[19] B. De Campos Vidal, M.L.S. Mello, Collagen type I amide I band infrared spectroscopy, Micron 42 (2011) 283–289, https://doi.org/10.1016/J.MICRON.2010.09.010.

[20] K. Belbachir, R. Noreen, G. Gouspillou, C. Petibois, Collagen types analysis and differentiation by FTIR spectroscopy, Anal. Bioanal. Chem. 395 (2009) 829–837, https://doi.org/10.1007/s00216-009-3019-y.

[21] A. Rebelo, J. Bizeau, L. Russo, A. Pandit, Glycan-Functionalized Collagen Hydrogels Modulate the Glycoenvironment of a Neuronal Primary Culture, Biomacromolecules. 21 (n.d.) 2681–2694. https://doi.org/10.1021/acs.biomac.0c00387.

[22] L. Russo, A. Sgambato, M. Lecchi, V. Pastori, M. Raspanti, A. Natalello, S.M. Doglia, F. Nicotra, L. Cipolla, Neoglucosylated collagen matrices drive neuronal cells to differentiate, ACS Chem. Neurosci. 5 (2014) 261–265, https://doi.org/10.1021/am200158y.

[23] J. Herna, Ndez-Ruiz, M.B. Arnao, A.N.P. Hiner, F. Garci, A-Ca, Novas, M. Acosta, Catalase-like activity of horseradish peroxidase : relationship to enzyme inactivation by H 2 O 2, Biochem. J. 354 (2001) 107–114.

[24] D.J. Danner, P.J. Brignac, D. Arceneaux, V. Patel, The oxidation of phenol and its reaction product by horseradish peroxidase and hydrogen peroxide, Arch. Biochem. Biophys. 156 (1973) 759–763, https://doi.org/10.1016/0003-9861(73)90329-9.

[25] S.F. Tang, X. Hou, Probing the toxic interactions between bisphenol A and glutathione S-transferase Phi8 from Arabidopsis thaliana, Ecotoxicol. Environ. Saf. 213 (2021), 112029, https://doi.org/10.1016/J.ECOENV.2021.112029.
[26] T.S. Raju, Glycosylation of proteins, Co□ post-translational modif, Ther. Antibodies Proteins (2019) 63–76, https://doi.org/10.1002/9781119053354.CH7.
[27] Q. Zhang, L. Li, Q. Lan, M. Li, D. Wu, H. Chen, Y. Liu, D. Lin, W. Qin, Z. Zhang, J. Liu, W. Yang, Protein glycosylation: a promising way to modify the functional properties and extend the application in food system, Crit. Rev. Food Sci. Nutr. 59 (2019) 2506–2533, https://doi.org/10.1080/10408398.2018.1507995.
[28] L. Russo, A. Gautieri, M. Raspanti, F. Taraballi, F. Nicotra, S. Vesentini, L. Cipolla, Carbohydrate-functionalized collagen matrices: design and characterization of a novel neoglycosylated biomaterial, Carbohydr. Res. 389 (2014) 12–17, https://doi.org/10.1016/J.CARRES.2013.11.008.
[29] M. Raspanti, E. Caravà, A. Sgambato, A. Natalello, L. Russo, L. Cipolla, The collaggrecan: synthesis and visualization of an artificial proteoglycan, Int. J. Biol. Macromol. 86 (2016) 65–70, https://doi.org/10.1016/J.IJBIOMAC.2016.01.051.
[30] A. Sgambato, L. Russo, M. Montesi, S. Panseri, M. Marcacci, E. Caravà, M. Raspanti, L. Cipolla, Different sialoside epitopes on collagen film surfaces direct mesenchymal stem cell fate, ACS Appl. Mater. Interfaces 8 (2016) 14952–14957, https://doi.org/10.1021/acsami.5b08270.